Textile-to-mortar bond behaviour in lime-based textile reinforced mortars

Ali Dalalbashi[1], Bahman Ghiassi [2*], Daniel V. Oliveira[3]

ABSTRACT

Lime-based textile-reinforced mortars (TRM) have recently found a growing interest for repair and strengthening of masonry and historical structures. Despite extensive experimental and numerical investigations performed in the last years on the performance of these composites, there is still a lack of fundamental understanding of the fabric-to-mortar bond behaviour (as one of the main mechanisms affecting the cracking and nonlinear response of these composites) and the parameters affecting that. This paper, aimed at addressing this gap, presents a comprehensive experimental and analytical investigation on how the test setup, embedded length, load rate, mortar age and fabric configuration affect the bond behaviour in lime-based TRMs. In total 160 pull-out tests are performed on a glass-based and a steel-based TRM commonly used for strengthening of masonry structures. The results contribute to standardization of the test procedures for characterization of the fabric-to-mortar bond behaviour, to fundamental understanding of this mechanism and to optimization of the design of these composites for enhancing their mechanical response.

Keywords: Textile reinforced mortars; TRM; FRCM; pull-out test; fabric-to-mortar bond behaviour; sustainable construction materials; strengthening;

[1] PhD Student, ISISE, University of Minho, Department of Civil Engineering, Azurém, 4800-058 Guimarães, Portugal. E-mail: alidalalbashi@gmail.com

[2]*Corresponding author, Assistant Professor, Centre for Structural Engineering and Informatics, Faculty of Engineering, University of Nottingham, Nottingham, United Kingdom. E-mail: bahman.ghiassi@nottingham.ac.uk

[3] Associate Professor, ISISE & IB-S, University of Minho, Department of Civil Engineering, Azurém, 4800-058 Guimarães, Portugal. E-mail: danvco@civil.uminho.pt

1 Introduction

Textile Reinforced Mortars (TRMs) have recently received extensive attention for externally bonded reinforcement of masonry structures. Compared to the conventional Fibre Reinforced Polymers (FRPs), TRMs have several advantages such as physical and mechanical compatibility with masonry, acceptable performance under high temperatures and lower installation costs [1–6].

TRMs are composed of continuous fabrics (unidirectional or bidirectional fabrics made of glass, steel, basalt, etc.) embedded in an inorganic matrix (lime-based or cement-based mortars). Due to better compatibility, lime-based mortars are the preferred choice for application to weak masonry and historical structures [7–10] and are the main subject of this study.

The mechanical properties of TRMs and their effectiveness in enhancing the performance of strengthened structural components are influenced by the properties of the mortar (TRM matrix), the properties of the fabric, the fibre-to-mortar bond behaviour and the TRM-to-masonry bond behaviour [1,11,12]. Although mechanical characterization of TRMs [2,3,13–15] or the bond between TRMs and masonry substrates [16–18] have been the subject of several experimental and numerical studies, the fabric-to-mortar bond behaviour, the main mechanism controlling the nonlinear response and cracking of TRM composites, has only received a limited attention especially in case of lime-based TRMs [1,19,20]. A fundamental understanding of this mechanism and the parameters affecting that, currently missing, is critical for development of TRM composites with enhanced mechanical properties and for fit-for-purpose design of TRMs for strengthening applications.

To address this need, this study presents a comprehensive experimental and analytical study on the role of test method, loading rate, fibre embedded length, fibre and mortar type, mortar

age and fabric configuration (longitudinal and bidirectional) on the pull-out response and bond-slip laws of lime-based TRMs. Two types of TRMs commonly used for strengthening of masonry structures, a steel-based and a glass-based, are selected for this purpose. The results presented and discussed in this paper contribute towards a fundamental understanding of the fabric-to-mortar bond behaviour as well as standardization of the bond characterization methods in lime-based TRM composites.

2 Experimental Program

The experimental campaign was aimed at evaluating the role of different parameters on the pull-out response of fibres embedded in lime-based mortars. The role of test setup, loading rate, embedded length, and mortar age on the pull-out response and the bond-slip laws are evaluated. Two commonly used fibre types (steel and glass) with their counterpart mortars (selected from the same producer) are used for this purpose. A summary of all the considered testing parameters is presented in Table 1.

2.1 Materials

Mortars employed in this study consisted of two commercial hydraulic lime-based mortars referred as M1 and M2 throughout this paper:

- Mortar M1: a commercially available high-ductility hydraulic lime mortar
- Mortar M2: a commercially available pure natural NHL 3.5 lime and mineral geo-binder

The reinforcing materials were glass and steel fibres, see Fig. 1. The glass fabric was a woven biaxial fabric mesh made of an alkali-resistance fibreglass (Mapegrid G220). Based on the technical datasheets provided by the manufacturer, this fabric has as tensile strength, elongation at breakage, and modulus of elasticity of 45 kN/m, 1.8 %, and 72 GPa, respectively.

The steel mesh was a unidirectional ultra-high tensile steel sheet (GeoSteel G600), with a density of 670 g/m^2, and an effective area of one cord (five wires) of 0.538 mm^2. Each steel fibre is made by twisting five individual wires together, three straight filaments wrapped by two filaments at a high twist angle, forming a uniform cord and a non-smooth surface that ensures a good bond with the matrix. Again, according to the technical datasheets, the tensile strength and elastic modulus are 2800 MPa and 190 GPa, respectively.

The TRM composites are developed using the fibre/mortar pairs from the same provider. This means that the glass fibres are used with the mortar M1 and the steel fibres with the mortar M2.

2.2 Material characterization tests

Mortar

Compressive and flexural tests were performed on mortar samples according to ASTM C109 [21] and EN 1015-11 [22], respectively. The changes in the mechanical properties of mortar with curing age were evaluated by performing the tests at the ages of 3, 7, 14, 28, 60, 90, and 180 days.

Compressive tests were performed on five cubic (50×50×50 mm^3) specimens at each age with a Lloyd testing machine under force-controlled conditions at the rate of 2.5 N/s. A pair of Teflon sheets with a layer of oil in between was placed between the specimens and the compression plates to reduce the friction near the boundaries (Fig. 2a).

Flexural tests were conducted on five prismatic (40×40×160 mm^3) specimens, at each age, following a three-point bending test scheme (Fig. 2b). The tests were performed with a Lloyd testing machine under force-controlled conditions at a rate of 10 N/s.

Fibres

Tensile strength and elastic modulus of the single rovings (cords) were measured by performing direct tensile tests. The tests were performed under displacement-controlled conditions at the rate of 0.3 mm/min (Fig. 2c). A 100 mm clip gauge, located at the centre of the specimens, was used to measure the fibres elongation during the tests.

2.3 Pull-out tests

2.3.1 Effect of test setup

Several tests setups have been used in the literature for characterization of the bond behaviour of fibres in cementitious matrices. These test setups can be roughly categorized into single-sided and double-sided (or pull-push and pull-pull tests). In pull-push tests, the yarns are embedded in the matrix from one side, and the tests are performed by fixing the top surface of the mortar and pulling the yarn from that surface [23–25]. In pull-pull tests, the yarn is embedded on both sides (with different embedded lengths) and the load is applied to the matrix following a tensile testing configuration [26,27]. The yarn is, therefore, pulled-out during the tests from the side with a smaller embedded length. There are extensive discussions on the advantages of each test setup. While pull-pull tests seem to better represent the actual stresses at the crack surface, the pull-push tests are easier to perform, are more reliable in terms of slip measurements, and the experimental results show a lower variation.

A comparison is made here between the pull-out response of fibres embedded in lime-based mortars tested under pull-pull and pull-push test schemes. Two pull-push and one pull-pull testing configuration, as shown in Fig. 3 are considered. Only steel fibres embedded in mortar M2 with an embedded length of 150 mm and cured for 60 days were used for this reason. Five specimens were tested with each test setup resulting in a total of 15 pull-out tests. A servo-hydraulic system with a maximum capacity of 25 kN was used for performing the tests. The tests (unless specified otherwise) were performed under displacement-controlled conditions

with reference to the internal LVDT of the system by pulling the roving/cord at a velocity of 1.0 mm/min.

Setup 1: Pull-push I

In this case, the specimens were composed of a single roving embedded in mortar cylinders with 75 mm diameter and 150 mm length. The tests were performed by blocking the specimens to a rigid frame and pulling the roving from their free end (from top) as shown in Fig. 3a. Aluminium tabs were glued to the cord's free end to facilitate gripping during the tests. The resultant load was measured by the load cell integrated in the testing machine, while the cord's slip was measured with an LVDT (20 mm range and 2-μm sensibility) attached to the cord at 20 mm distance from the mortar edge (or fibre loaded end). This test setup required application of a small preload to facilitate attachment of the LVDT. The slip was calculated by reducing the elastic elongation of the unbonded roving from the LVDT measurements.

Setup 2: Pull-push II

Due to the complexities associated with measurement of the slip in pull-push I test setup, the specimens' geometry and test details were modified in pull-push II test setup. Here, the specimens were made of single roving (or cords) embedded in a prismatic mortar with the dimensions of 150×125×16 mm^3 (Fig. 4a). The free length of the cords were embedded in an epoxy resin block over a length of 200 mm and with a rectangular cross-sectional area of 10×16 mm^2. This block, also used in [28], facilitates gripping, facilitates slip measurements in one-sided pull-out tests and protects the fabric from premature failure. Here, a U-shape steel support was utilized for supporting the specimens (Fig. 3b). A mechanical clamp (similar to pull-push I) was used to grip the epoxy resin from the top and two LVDTs were located at both sides of the epoxy block, at the vicinity of the mortar edge, to record the slip during the

tests. Again, the tests were performed by pulling the epoxy block with a displacement rate of 1.0 mm/min.

Setup 3: Pull-pull

In this test setup, the mortar was gripped from the bottom with a fixed mechanical gripping system and the fabric was pulled from top, as illustrated in Fig. 3c. The specimens had a similar geometry as the pull-push II specimens, but were made longer (with dimensions of 250×125×16 mm^3) to allow gripping of the mortar from the bottom. The mortar was reinforced with fabric in the gripping area to avoid cracking of the samples during the tests. Again, the free length of the cords were embedded in an epoxy resin block over a length of 200 mm and with a rectangular cross-sectional area of 10×16 mm^2. Two LVDTs were mounted on the testing block with the supports placed on the mortar edge to measure the slip during the tests.

,Againthe tests were performed by pulling the epoxy block with a displacement rate of 1.0 mm/min.

2.3.2 Effect of embedded length

To evaluate the role of fabric embedded length on the pull-out response, specimens were prepared by embedding a single roving/cord with different lengths of 50, 100, 150, and 200 mm for steel-based TRMs and 50, 75, and 100 mm for glass-based TRMs. These lengths were chosen based on the experimental results reported by Ghiassi et al. [1]. Five specimens were tested for each material and bond length resulting in a total of 20 steel-based TRM specimens and a total of 15 glass-based TRM specimens. These tests were performed after 60 days curing and using the pull-push II test setup under the loading and boundary conditions explained in sec. 2.3.1.

2.3.3 Effect of loading rate

To evaluate the role of load rate on the pull-out response, glass-based and steel-based TRM specimens with 50 mm and 150 mm embedded length, respectively, were tested (using the pull-push II testing configuration) under four different loading rates of 0.3 mm/min, 1.0 mm/min, 3.0 mm/min and 5.0 mm/min. 1.0 mm/min is the common loading rate used for performing pull-out tests and is believed to ensure a quasi-static testing condition. 0.3 mm/min is used here to evaluate if the assumption stated in the previous sentence is accurate. This loading rate is also a common loading rate usually used for performing debonding shear tests in TRM composites [1,2]. 3.0 mm/min and 5.0 mm/min are chosen to investigate if the pull-out results are sensitive to these higher loading rate.

The embedded length chosen for the steel-based TRM is corresponding to the effective embedded length, sec. 3.3. In case of glass-based TRM, the effective bond length is between 50 mm and 75 mm, see sec. 3.3. 50 mm embedded length is chosen here to avoid occurrence of a mix failure mode in the specimens (see sec. 3.3.2 on failure modes of the specimens in different embedded lengths). Again, five specimens were prepared and tested (At 60 days mortar curing age) for each loading rate and TRM type leading to a total of 40 specimens.

2.3.4 Effect of mortar age

Both glass-based and steel-based specimens are tested (using the pull-push II testing configuration) at mortar ages of 15, 30, 90, and 180 days to evaluate how the mortar age affect the pull-out response of TRM composites. Again, the specimens were made with embedded lengths of 50 mm for glass-based TRM and 150 mm for steel-based TRM. Four specimens were prepared and tested at each mortar age resulting in a total of 20 specimens for each TRM type.

2.3.5 Effect of fabric configuration

Three cases were considered for each TRM type to understand the role of fabric configuration on the pull-out response.

For the glass-based TRM, a bidirectional fabric, the specimens consisted of a single roving (Fig. 4d), single roving + transverse elements (Fig. 4e), and two rovings with transverse elements (Fig. 4f) embedded in mortar for 50 mm. This is chosen to investigate the role of transverse roving on the pull-out response of the specimens. The transverse elements had a total length of 50 mm.

For the steel-based TRM, which was a unidirectional fabric, the specimens consisted of a single cord, two cords, and four cords embedded in mortar for 150 mm (see Fig. 4a-c) to evaluate how role of number of cords on the pull-out response. Five specimens were prepared in each case and tested at 60 days resulting in a total of 30 specimens.

3 Experimental results and discussion

3.1 Material properties

Mortar

The changes in the mortars' mechanical properties with age are presented in Table 2 and Fig. 5. It can be observed that although the peak compressive strength of both mortars is similar (8.31 MPa for M1 and 9.53 MPa for M2), this value is reached in different ages. Mortar M2 reaches the peak compressive strength in the first 30 days, which is followed by decrement of the strength until 180 days. Meanwhile, mortar M1 reaches its peak compressive strength in 60 days after which a slight decrement of the strength is observed.

As for flexural strength, mortar M2 reaches its peak strength in the first 30 days, after which the changes in the strength are negligible. The flexural strength of mortar M1, however, shows a continuous increase until 180 days. Mortar M1 shows a higher flexural strength (5.1 MPa

for M1 compared to 2.62 MPa for M2), although having a lower compressive strength. This indicates a more ductile response of this mortar which can be due to the existence of short fibres in the mortar powder.

Fibre

The experimental stress-strain curves obtained from direct tensile tests on single roving/cords are presented in Fig. 6. The results show an average tensile strength of 2972 MPa, Young's modulus of 189.34 GPa, and strain corresponding to the peak stress of 1.88 % for steel fibres. These values are obtained as 875 MPa (0.7715 kN) and 65.94 GPa, and 1.77 %, respectively, for the glass roving. It can be observed that, despite the tensile strength of the glass fibres, the experimental values are comparable to those reported in the technical datasheets, see sec. 2.1. The obtained tensile strength of the glass roving is equivalent to 31.63 kN/m that is about 30% smaller than the one reported in the technical datasheets.

3.2 Effect of test setup

The experimental envelope and average force-slip curves obtained from different test setups are shown in Fig. 7(a). It can be seen that the variation of experimental results is highest in the specimens tested under pull-pull I testing configuration.

The main characteristics of the pull-out curves including the peak load, the slip corresponding to the peak load, the toughness (defined as the area under the force-slip curve), and the initial stiffness of the pull-out curves are extracted from the average pull-out curves and presented in Table 3. Due to the lack of a standard criterion for calculation of the toughness, this parameter has been reported at different slip values of 1 mm, 4 mm and 8 mm. It can be seen that all these parameters are higher in the specimens tested in pull-pull test setup compared to the specimens tested in the pull-push test setups. This is due to the differences in the boundary

conditions and distribution of the stresses in the specimens and have also been previously observed in the pull-out of fibres from cementitious matrices [29].

In pull-push tests, the average pull-out curves obtained from pull-push I and pull-push II are similar. Despite this similarity, the specimens tested under pull-push II configuration show a higher initial stiffness and lower toughness which is due to the more robust way of measuring the cord slip in these specimens. As explained before, in pull-push I test setup, the LVDTs are mounted on the cord at a distance from the mortar edge. In this case, the slip values are obtained by reducing the elastic deformation of the cord from LVDT which can be a source of error in the measurements. In pull-push II test setup, however, embedment of the free length of the cords in the epoxy block allowed attachment of the LVDTs at the vicinity of the mortar edge and thus direct measurement of the slip values from LVDTs.

With the aim of the analytical modelling approach proposed by Banholzer et al. [30,31], the roving (cord)-to-mortar bond-slip laws are obtained from the experimental pull-out curves and presented in Fig. 7(b) (here A_m is the effective mortar area, E_m is the mortar elastic modulus, A_f is the effective fibre area and E_f is the roving elastic modulus). As expected, the bond-slip laws show a higher initial stiffness, bond strength and frictional stress in pull-pull tests compared to that of pull-push tests. Interestingly, the bond-slip laws extracted from the pull-push I and II test setups do not show any significant difference.

As mentioned before, although it is claimed that pull-pull tests represent the stress and boundary conditions at the crack surface in a more realistic way, pull-push tests are easier to perform and produce a smaller variation in the experimental results. For this reason, the modified pull-push test method (pull-push II) is used hereafter.

3.3 Effect of embedded length

The average load-slip curves of specimens with different embedded lengths are presented in Fig. 8 and Fig. 9.

3.3.1 Steel-based TRM

The failure mode of the specimens was slippage of the fibre from the mortar in all specimens, except for three specimens in which mortar cracked during the tests. It can be noted that the maximum obtained pull-out load is lower than the tensile strength of the steel fibres in all embedded lengths, Fig. 8. The pull-out curves show that once the peak load is reached, a sudden drop occurs in the force followed by a slip hardening behaviour and then softening of the pull-put curves. This slip hardening behaviour, visible in embedded length of ≥100 mm, is also reported in the literature [32,33] and increases with increment of the embedded length. The pull-out response after the peak load is mainly affected by the frictional stresses between the cord and the matrix. A high frictional stress leads to a slip hardening response, while a low frictional stress leads to a slip softening behaviour [34,35]. For steel-based TRMs tested in this study, the geometrical features of the steel cords (twisted nature) has led to development of high frictional stresses between the cord and the mortar and therefore the observed slip hardening response.

The changes of the average peak load, the slip corresponding to the peak load, and the initial stiffness with embedded length are also presented in Fig. 8. It can be observed the peak load increases until 150 mm embedded length and does not change significantly thereafter. This suggests that the effective bond length of this TRM composite is in the range of 150-200 mm, also in agreement with [1,16]. At the same time, the initial stiffness of the pull-out curves is decreased and the slip corresponding to the peak load is increased with increment of the embedded length, a phenomenon that has also been reported previously [32,36–40].No

specific correlation between the variation in the eperimental results and embedded length can be observed. -The bondslip laws ,Fig. 10 ,show that with increasing the embedded length, the stiffness and bond strenght of the extracted bond-slip laws decreases.

3.3.2 Glass-based TRM

Again, the test results indicate the significant effect of the embedded length on the bond behaviour. In this case, the failure mode of the specimens changed from fibre slippage to fibre tensile rupture with increasing the embedded length from 50 mm to 100 mm. The roving slippage from the mortar was observed in the specimens with embedded length of 50 mm. Specimens with embedded length of 75 mm showed an initial slippage followed by tensile rupture of the roving. Finally, specimens with embedded length of 100 mm failed due to tensile rupture of the roving. The effect of failure mode on the pull-out curves is clear. It can be seen that the pull-out curves in 50 mm and 75 mm embedded lengths are similar to the pull-out curves obtained from steel-based TRMs (the pull-out curves show a first peak load followed by a drop and then a slip hardening response). The results suggest that the effective bond length in this system is between 50 mm and 75 mm that is about half of the steel-based TRM tested in previous section.

Again, by increasing the embedded length, the peak load increases until occurrence of the roving's rupture. The rupture occurs at a load level close to the roving tensile strength experimentally obtained in direct tensile tests showing full utilization of the nominal fabric capacity. In contrast to the steel fibres, the changes of the slip corresponding to the peak load and initial stiffness of the pull-out curves do not follow a clear trend. This is mainly due to the changes of the failure mode with increasing the embedded length.

3.4 Effect of loading rate

The average pull-out curves of both TRM types tested under different loading rates is shown in Fig. 11, Table 4 and Table 5. Overall, the role of loading rate on the pull-out response is clearly dependent on the TRM type. In both TRM types, increasing the loading rate has led to increment of the initial stiffness and peak load in the pull-out curves. This effect is more obvious in glass-based TRM studied here.

In steel-based TRM, Fig. 11a, the general shape of the load-slip curves and failure mode of the samples (always fibre slippage) does not change with the load rate and consist of the typical initial elastic stage, a drop after initiation of the debonding, a strain hardening stage and finally a softening stage. The average load-slip curves of the specimens tested at the loading rate of 0.3 mm/min is clearly below the other specimens. Meanwhile, the pull-out curves of the specimens tested at loading rates of 1.0 mm/min, 3.0 mm/min and 5.0 mm/min does not show a significant difference.

On the other hand, in glass-based TRMs, there is a clear differences between the average pull-out curves of the specimens tested under the loading rate of 0.3 mm/min and 1.0 mm/min and the specimens tested under the loading rate of 3.0 mm/min and 5.0 mm/min, Fig. 11b. While the failure mode of all the specimens have been slippage of the roving from the mortar, the general shape of the pull-out curves has changed. The specimens tested under the loading rate of 3.0 mm/min and 5.0 mm/min show a larger initial stiffness, a higher peak load, a larger slip hardening after the peak load and consequently a significantly larger toughness.

A commonly neglected but important consideration in pull-out (also shear debonding) tests is the speed at which the tests are performed (usually controlled by the clamps movements or internal LVDT of the hydraulic jacks) might be different than the rate of slip induced in the

samples. This difference, if significant, should be considered when experimental results from different databases are compared.

A look at the slip rates (the rate of slip recorded by the LVDTs mounted at the edge of the embedded length) induced in the specimens tested in this study, Fig. 12, shows that, despite embedment of the free fabric in an epoxy resin block, the slip rate at the interface of steel-based and glass-based TRMs is slightly different.

3.5 Effect of mortar age

3.5.1 Steel-based TRM

The average pull-out response of steel-based TRMs tested at different mortar ages are shown in Fig. 13 and Fig. 14. The summary of the results are also presented in Table 6. The pull-out curves show the typical three stage behaviour at all ages (see Fig. 13): linear, nonlinear, and dynamic stage. The linear elastic range terminates when the first debonding at the interface occurs followed by a concave-downward shape in the pull-out curves until reaching the peak load [41]. After the peak load, which corresponds to full debonding along the embedded length, a sudden drop of the load can be observed showing that the adhesive forces are larger than the frictional forces in this system [42]. The pull-out curves, then, show a slip hardening behaviour (forming a second peak load) and then a softening response until the end of the tests. The average pull-out curves show a slight decrease of the peak load and toughness after 30 days, very similar to the observed changes in the mechanical properties of the mortar M2 (Fig. 2), which might be due to shrinkage cracking of the samples (no visible cracks were observed). At the same time, the slip corresponding to the first peak load is almost constant and the initial stiffness decreases with time.

The extracted bond-slip laws, Fig. 14b, show that the bond-slip law obtained from the 30 days tests has the highest bond strength and stiffness. The bond-slip laws obtained at 90 and 180

days are very similar and seem to be more representative of the long-term performance of the steel-based TRMs studied here.

3.5.2 Glass-based TRM

The evolution of the average pull-out curves of the glass-based TRMs with mortar age are presented in Fig. 15 and Fig. 16. The summary of the main characteristics of the pull-out curves in different ages are also presented in Table 7. It can be seen that while the slip corresponding to the peak load is relatively constant, the peak load, toughness and initial stiffness of the pull-out curves increase with time until 180 days.

A significant change can be observed in the pull-put curves with mortar age. At the mortar ages of 15 and 30 days, after complete debonding (at peak load), a descending trend in the pull-out force can be observed. In contrast, at the age of 90 and 180 days, the pull-out force increases after complete debonding showing a slip hardening behaviour. The changes in the peak loads, again, is in-line with the observed changes of mechanical properties of mortar M1 (Fig. 2, the flexural strength of mortar M1 continuously increased until 180 days).

As expected, the bond-slip laws obtained from the pull-out curves, Fig. 16b, show a significant effect of mortar age in this TRM system. Again, the results show that 90 days of curing seems to be the minimum required age for evaluating the bond behaviour in this case.

3.6 Effect of fabric configuration

3.6.1 Steel-based TRM

The average pull-out curves and summary of the results obtained from steel-based TRMs with different configurations are shown in Fig. 17 and Table 8. The results are presented in terms of the applied load per fibre (load divided by the number of fibres) versus slip to facilitate comparison between different configurations. Interestingly, the peak load, slip corresponding to the peak slip and toughness decrease with increasing the number of cords. This has led to a

lower bond strength, stiffness and residual strength in bond-slip laws of specimens with a larger number of cords, Fig. 17(b). This "group effect" shows the importance of consideration of the fabric geometry on the pull-out tests and on characterization of bond behaviour in TRM composites. Understanding the minimum number of cords or the minimum distance between longitudinal cords from which this group effect is diminished, not enabled by this experimental results, can be interesting in design of TRM composites with enhanced mechanical properties and should be followed in future studies.

3.6.2 Glass-based TRM

The average pull-out curves and summary of the results obtained from glass-based TRMs with different configurations are shown in Fig. 18 and Table 9. The results are presented in terms of the applied load per fibre (load divided by the number of fibres) versus slip to facilitate comparison between different configurations. Again, the "group effect" is clear in the obtained experimental results. It can be observed that the transverse elements have a significant effect on the pull-out response (mainly on the post peak response and toughness) and the bond-slip laws in this TRM composite. Interestingly, the bond behaviour in the "group" and "single roving + transverse" specimens is similar. This is in contrast to the behaviour observed in steel-based TRMs, and shows that the longitudinal fabrics in this system do not impose any group effects which is probably due to the distance between the grids (25 mm). Clearly, the role of transverse elements on the bond behaviour as a function of junction types (welded, woven, non-woven, etc.) is a subject that needs to be addressed in future investigations.

4 Conclusions

A comprehensive experimental study was presented in this paper on the role of different parameters on the pull-out response of steel and glass fibres embedded in lime-based matrices. The effect of test setup, embedded length, loading rate, mortar age and fibre configuration on

the pull-out response and bond-slip laws of 160 specimens was investigated and discussed. The conclusions drawn from the analysis of the obtained experimental results are listed as follows:

- A conventional pull-push, a modified pull-push and a modified pull-pull test setup were developed to investigate the role of test setup on the pull-out response of TRM composites. The results showed that the bond-slip laws obtained from pull-pull tests show a higher bond strength and stiffness compared to pull-push tests. While pull-pull tests seem to better represent the stress state at the crack surfaces, pull-push tests are easier to perform and produce a smaller variation in the experimental results. For this reason, the modified pull-push test setup was further used in this study to evaluate the role of other parameters on the pull-out response of TRM composites.
- The effect of embedded length was investigated by testing steel-based TRMs with 50, 100, 150, and 200 mm embedded length and glass-based TRMs with 50, 75 and 100 mm embedded length. In the steel-based TRMs, the failure mode was slippage in all embedded lengths. With increment of the embedded length, the initial stiffness of the pull-out curves and the slip corresponding to the peak load increased independent from the embedded length. It was also observed that the peak load reached its maximum value at a bonded length of 150 mm. These results suggest that the effective bond length in this system is around 150 mm. In glass-based TRMs, the failure mode changed from fibre slippage (in 50 mm) to mixed slippage and roving rupture (in 75 mm) and roving rupture (in 100 mm). This suggests that the effective bond length in this system is between 50 mm and 75 mm. The bond-slip laws extracted from pull-out curves showed a decreasing bond strength and stiffness with increment of the embedded length even when the length was larger than effective embedded length.

- The effect of load rate was found to be dependent on the TRM system used. In the steel-based TRM, the tests performed at 0.3 mm/min produced the lowest results (about 20% lower). Meanwhile, the results obtained from the tested performed at higher rates (1.0 mm/min, 3.0 mm/min and 5.0 mm/min), did not show any significant rate dependency (average curves). In the glass-based TRM, the average results obtained from the test rates of 0.3 mm/min and 1.0 mm/min were very similar and significantly lower than the results obtained from higher load rates. Additionally, it was observed that glass and steel-based TRMs tested under the same loading rates and with the same fibre free length (outside of the embedded length) experienced a slightly different slip rates at the vicinity of the mortar edge. This observation is of critical importance and shows comparison of results between different TRM types should be done with special care.
- Mortar age was found to be a critical factor in the pull-out response of lime-based TRMs. In particular, the steel-based TRM studied here showed a maximum bond response at 30 days followed by a decrement of the bond strength and stiffness until 90 days. After this age, the changes in the bond behaviour were insignificant. In glass-based TRM, a continuous enhancement of the bond behaviour was observed until 180 days of curing. These results show the 30 days curing age, commonly used for cementitious mortars, is too short for evaluating the bond behaviour in lime-based TRMs. This age dependency seems to be highly dependent on the mortar type. Due to the large variety of available lime matrices, it is difficult to propose a generic curing time that is representative of their long-term response for performing the pull-out tests. Evaluating the hydration degree of the mortar at the interface is therefore a critical factor. As an alternative, the changes of the flexural strength of the mortar was found

to be a good indicator for estimating the suitable curing age for evaluating the mechanical properties and bond response of these composites.

- The pull-out response of steel-based TRM (unidirectional fabric) studied here was found to be influenced by the number of tested cords (the larger the number of cords the lower the bond strength was found) showing a sort of "group effect" in the results. This is believed to be influenced by the distance between the longitudinal cords. The minimum distance between the cords or the minimum number of cords to be tested for diminishing the group effect should be investigated in future studies. In glass-based TRM (bidirectional fabric) studied here, this group effect as not observed. However, the transverse elements had a significant effect of on the bond response of these composites.

The results contribute to standardization of the test procedures for characterization of the fabric-to-mortar bond behaviour, to fundamental understanding of this mechanism and to optimization of the design of these composites for enhancing their mechanical response. These results also show the importance of the investigated parameters and the need for further investigations on the fabric-to-mortar bond behaviour in TRM composites.

5 Acknowledgements

This work was partly financed by FEDER funds through the Competitivity Factors Operational Programme (COMPETE) and by national funds through the Foundation for Science and Technology (FCT) within the scope of project POCI-01-0145-FEDER-007633. The support to the first author through grant SFRH/BD/131282/2017 is acknowledged.

6 References

[1] B. Ghiassi, D. V Oliveira, V. Marques, E. Soares, H. Maljaee, Multi-level characterization of steel reinforced mortars for strengthening of masonry structures, Mater. Des. 110 (2016) 903–913. doi:10.1016/j.matdes.2016.08.034.

[2] M. Leone, M.A. Aiello, A. Balsamo, F.G. Carozzi, F. Ceroni, M. Corradi, M. Gams, E. Garbin, N.

Gattesco, P. Krajewski, C. Mazzotti, D. Oliveira, C. Papanicolaou, G. Ranocchiai, F. Roscini, D. Saenger, Glass fabric reinforced cementitious matrix: Tensile properties and bond performance on masonry substrate, Compos. Part B Eng. 127 (2017). doi:10.1016/j.compositesb.2017.06.028.

[3] C. Caggegi, F.G. Carozzi, S. De Santis, F. Fabbrocino, F. Focacci, Ł. Hojdys, E. Lanoye, L. Zuccarino, Experimental analysis on tensile and bond properties of PBO and aramid fabric reinforced cementitious matrix for strengthening masonry structures, Compos. Part B Eng. 127 (2017). doi:10.1016/j.compositesb.2017.05.048.

[4] S. De Santis, F. Ceroni, G. de Felice, M. Fagone, B. Ghiassi, A. Kwiecień, G.P. Lignola, M. Morganti, M. Santandrea, M.R. Valluzzi, A. Viskovic, Round Robin Test on tensile and bond behaviour of Steel Reinforced Grout systems, Compos. Part B Eng. 127 (2017) 100–120. doi:10.1016/j.compositesb.2017.03.052.

[5] C.G. Papanicolaou, T.C. Triantafillou, M. Papathanasiou, K. Karlos, Textile-reinforced mortar (TRM) versus FRP as strengthening material of URM walls: in-plane cyclic loading, Mater. Struct. 40 (2007) 1081–1097. doi:10.1617/s11527-006-9207-8.

[6] T.C. Triantafillou, C.G. Papanicolaou, Textile reinforced mortars (TRM) versus fiber reinforced polymers (FRP) as strengthening materials of concrete structures, Spec. Publ. 230 (2005) 99–118.

[7] S. Barr, W.J. Mccarter, B. Suryanto, Bond-strength performance of hydraulic lime and natural cement mortared sandstone masonry, Constr. Build. Mater. 84 (2015) 128–135. doi:10.1016/j.conbuildmat.2015.03.016.

[8] V. Pavlík, M. Uzáková, Effect of curing conditions on the properties of lime, lime–metakaolin and lime–zeolite mortars, Constr. Build. Mater. 102 (2016) 14–25. doi:10.1016/j.conbuildmat.2015.10.128.

[9] J. Lanas, J.L. Perez Bernal, M.A. Bello, J.I. Alvarez, Mechanical properties of masonry repair dolomitic lime-based mortars, Cem. Concr. Res. 36 (2006) 951–960. doi:10.1016/j.cemconres.2005.10.004.

[10] C. Groot, RILEM TC 203-RHM: Performance requirements for renders and plasters, Mater. Struct. 45 (2012) 1277–1285. doi:10.1617/s11527-012-9916-0.

[11] G. Ferrara, M. Pepe, E. Martinelli, R. Dias Tolêdo Filho, Influence of an impregnation treatment on the morphology and mechanical behaviour of flax yarns embedded in hydraulic lime mortar, Fibers. 7 (2019) 30. doi:10.3390/fib7040030.

[12] B. Mobasher, Mechanics of Fiber and Textile Reinforced Cement Composites, Taylor & Francis Group, London- New York, 2012.

[13] P. Larrinaga, C. Chastre, J.T. San-José, L. Garmendia, Non-linear analytical model of composites based on basalt textile reinforced mortar under uniaxial tension, Compos. Part B Eng. 55 (2013) 518–527. doi:10.1016/j.compositesb.2013.06.043.

[14] A. Formisano, E.J. Dessì, R. Landolfo, Mechanical-physical experimental tests on lime mortars and bricks reinforced with hemp, in: Int. Conf. Comput. Methods Sci. Eng. 2017, ICCMSE 2017, Greece, 2017. doi:10.1063/1.5012363.

[15] H. Akbari Hadad, A. Nanni, U.A. Ebead, A. El Refai, Static and fatigue performance of FRCM-strengthened concrete beams, J. Compos. Constr. 22 (2018). doi:10.1061/(ASCE)CC.1943-5614.0000868.

[16] A. Razavizadeh, B. Ghiassi, D. V. Oliveira, Bond behavior of SRG-strengthened masonry units: Testing and numerical modeling, Constr. Build. Mater. 64 (2014) 387–397. doi:10.1016/j.conbuildmat.2014.04.070.

[17] L. Ascione, G. De Felice, S. De Santis, A qualification method for externally bonded Fibre Reinforced Cementitious Matrix (FRCM) strengthening systems, Compos. Part B Eng. 78 (2015) 497–506. doi:10.1016/j.compositesb.2015.03.079.

[18] L.H. Sneed, T. D'Antino, C. Carloni, Investigation of bond behavior of polyparaphenylene benzobisoxazole fiber-reinforced cementitious matrix composite-concrete interface, ACI Mater. J. 111 (2014). doi:10.14359/51686604.

[19] A. Dalalbashi, B. Ghiassi, D.V. Oliveira, A. Freitas, Effect of test setup on the fiber-to-mortar pullout response in TRM composites: experimental and analytical modeling, Compos. Part B Eng. 143 (2018) 250–268. doi:10.1016/j.compositesb.2018.02.010.

[20] A. Dalalbashi, B. Ghiassi, D.V. Oliveira, A. Freitas, Fiber-to-mortar bond behavior in TRM composites: effect of embedded length and fiber configuration, Compos. Part B Eng. 152 (2018) 43–57. doi:10.1016/j.compositesb.2018.06.014.

[21] ASTM C109/C109M-05, Standard test method for compressive strength of hydraulic cement mortars (Using 2-in. or [50-mm] Cube Specimens), 2005. doi:10.1520/C0109_C0109M-05.

[22] BS EN 1015-11, Methods of test for mortar for masonry. Determination of flexural and compressive strength of hardened mortar, 1999.

[23] J. Shannag, R. Brincker, W. Hansen, Pullout behavior of steel fibers from cement-based composites, Cem. Concr. Res. 27 (1997) 925–936. doi:10.1016/S0008-8846(97)00061-6.
[24] S. Sueki, C. Soranakom, B. Mobasher, M. Asce, A. Peled, Pullout-slip response of fabrics embedded in a cement paste matrix, J. Mater. Civ. Eng. 19 (2007) 718–728. doi:10.1061/(ASCE)0899-1561(2007)19:9(718).
[25] M. Baena, L. Torres, A. Turon, M. Llorens, C. Barris, Bond behaviour between recycled aggregate concrete and glass fibre reinforced polymer bars, Constr. Build. Mater. 106 (2016) 449–460. doi:10.1016/j.conbuildmat.2015.12.145.
[26] L. Huang, Y. Chi, L. Xu, P. Chen, A. Zhang, Local bond performance of rebar embedded in steel-polypropylene hybrid fiber reinforced concrete under monotonic and cyclic loading, Constr. Build. Mater. 103 (2016) 77–92. doi:10.1016/j.conbuildmat.2015.11.040.
[27] Y. Li, J. Bielak, J. Hegger, R. Chudoba, An incremental inverse analysis procedure for identification of bond-slip laws in composites applied to textile reinforced concrete, Compos. Part B Eng. 137 (2018) 111–122. doi:10.1016/j.compositesb.2017.11.014.
[28] B. Banholzer, Bond of a strand in a cementitious matrix, Mater. Struct. 39 (2006) 1015–1028. doi:10.1617/s11527-006-9115-y.
[29] L. Zhou, Y. Mai, C. Baillie, Interfacial debonding and fibre pull-out stresses, J. Mater. Sci. 29 (1994) 5541–5550. doi:10.1007/BF00349945.
[30] B. Banholzer, Analytical simulation of pull-out tests- the direct problem, Cem. Concr. Compos. 27 (2005) 93–101. doi:10.1016/j.cemconcomp.2004.01.006.
[31] B. Banholzer, W. Brameshuber, W. Jung, Analytical evaluation of pull-out tests-The inverse problem, Cem. Concr. Compos. 28 (2006) 564–571. doi:10.1016/j.cemconcomp.2006.02.015.
[32] P. Robins, S. Austin, P. Jones, Pull-out behaviour of hooked steel fibres, Mater. Struct. 35 (2002) 434–442. doi:10.1007/BF02483148.
[33] M. Butler, V. Mechtcherine, S. Hempel, Experimental investigations on the durability of fibre-matrix interfaces in textile-reinforced concrete, Cem. Concr. Compos. 31 (2009) 221–231. doi:10.1016/j.cemconcomp.2009.02.005.
[34] E.-H. Yang, S. Wang, Y. Yang, V.C. Li, Fiber-Bridging Constitutive Law of Engineered Cementitious Composites, J. Adv. Concr. Technol. 6 (2008) 181–193. doi:10.3151/jact.6.181.
[35] V.C. Lin, Z.; Li, Crack Bridging in Fiber Reinforced Cementitious Composites with Slip-Hardening Interfaces, J. Mech. Phys. Solids. 45 (1997) 763–787. doi:10.1016/S0022-5096(96)00095-6.
[36] N.W. Portal, I.F. Perez, L.N. Thrane, K. Lundgren, Pull-out of textile reinforcement in concrete, Constr. Build. Mater. 71 (2014) 63–71. doi:10.1016/j.conbuildmat.2014.08.014.
[37] M. Tuyan, H. Yazıcı, Pull-out behavior of single steel fiber from SIFCON matrix, Constr. Build. Mater. 35 (2012) 571–577. doi:10.1016/j.conbuildmat.2012.04.110.
[38] M.G. Alberti, A. Enfedaque, J.C. Gálvez, A. Ferreras, Pull-out behaviour and interface critical parameters of polyolefin fibres embedded in mortar and self-compacting concrete matrixes, Constr. Build. Mater. 112 (2016) 607–622. doi:10.1016/j.conbuildmat.2016.02.128.
[39] B. Wang, H. Jin, T. Man, Q. Wang, Study on the mechanical property of textile reinforced self-stressing concrete sheets, Constr. Build. Mater. 107 (2016) 1–10. doi:10.1016/j.conbuildmat.2015.12.167.
[40] X.B. Zhang, H. Aljewifi, J. Li, Failure behaviour investigation of continuous yarn reinforced cementitious composites, Constr. Build. Mater. 47 (2013) 456–464. doi:10.1016/j.conbuildmat.2013.05.022.
[41] T. D'Antino, F.G. Carrozzi, P. Colombi, C. Poggi, A New Pull-Out Test to Study the Bond Behavior of Fiber Reinforced Cementitious Composites, Key Eng. Mater. 747 (2017) 258–265. doi:10.4028/www.scientific.net/KEM.747.258.
[42] V.C. Li, H.C. Wu, Y.W. Chan, Interfacial property tailoring for pseudo strain- hardening cementitious composites, Adv. Technol. Des. Fabr. Compos. Mater. Struct. (1995) 261–268.

Figures

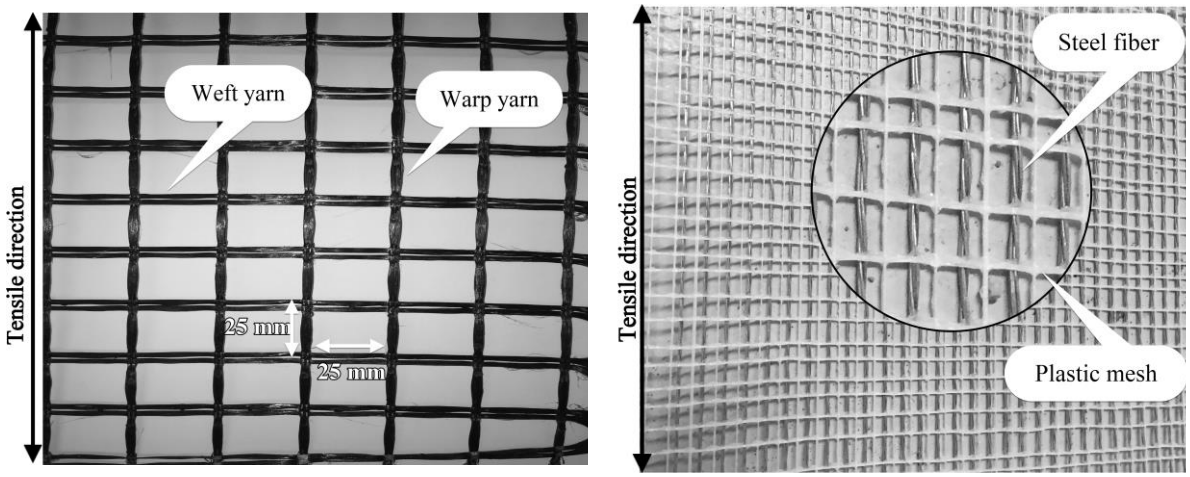

(a) (b)

Fig. 1. Fabrics employed in this study.

(a) (b) (c)

Fig. 2. Mechanical characterization tests: (a) mortar compressive test; (b) mortar flexural test; (c) fibre direct tensile test.

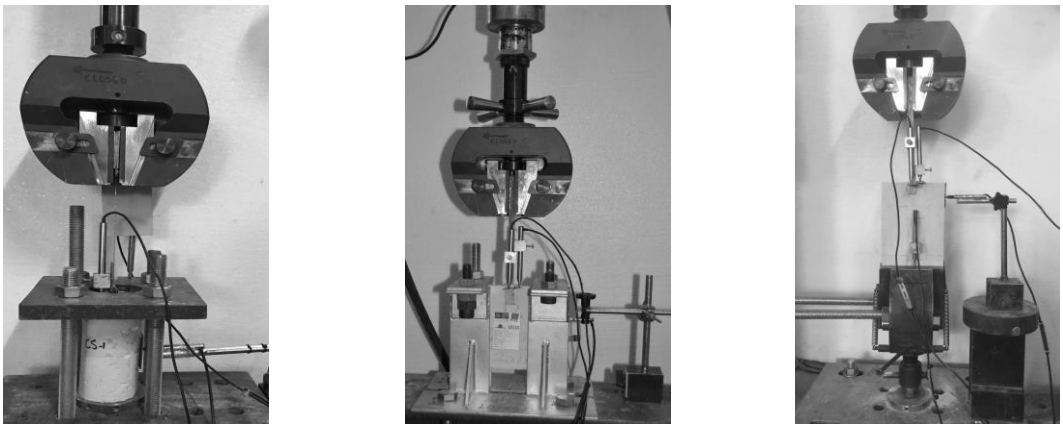

(a) (b) (c)

Fig. 3. Test setups and instrumentation used for pull-out tests: (a) pull-push I; (b) pull-push II; (c) pull-pull.

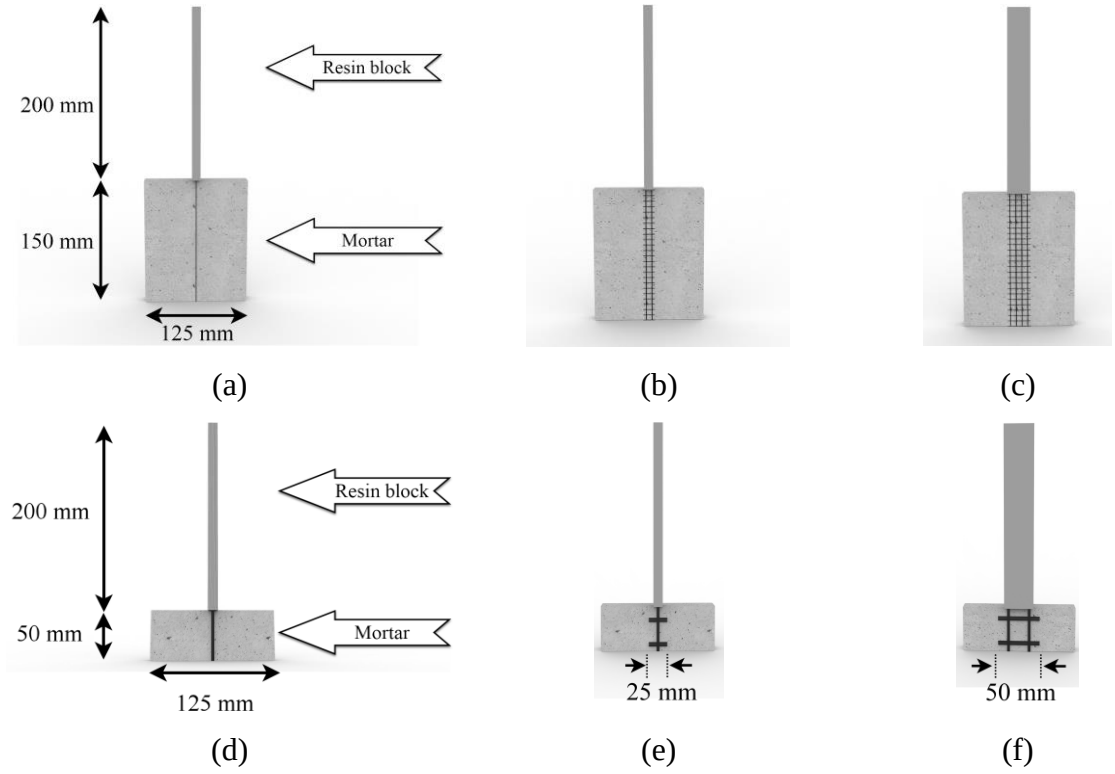

Fig. 4. Geometrical configuration of the pull-out specimens: (a) single cord steel-based TRM; (b) two cords steel-based TRM; (c) four cords steel-based TRM; (d) single roving glass-based TRM; (e) single roving glass-based TRM + transverse elements; (f) group glass-based TRM.

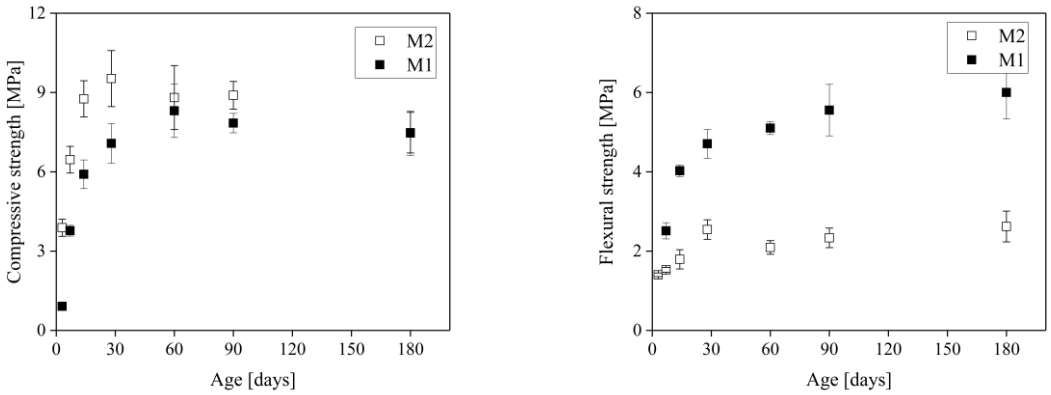

(a) (b)

Fig. 5. Changes of mechanical properties of mortar with time: (a) compressive strength; (b) flexural strength.

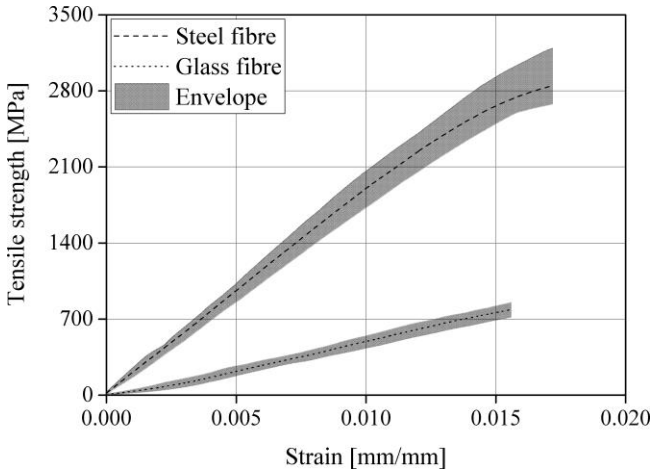

Fig. 6. Tensile behaviour of single dry steel cord and glass roving.

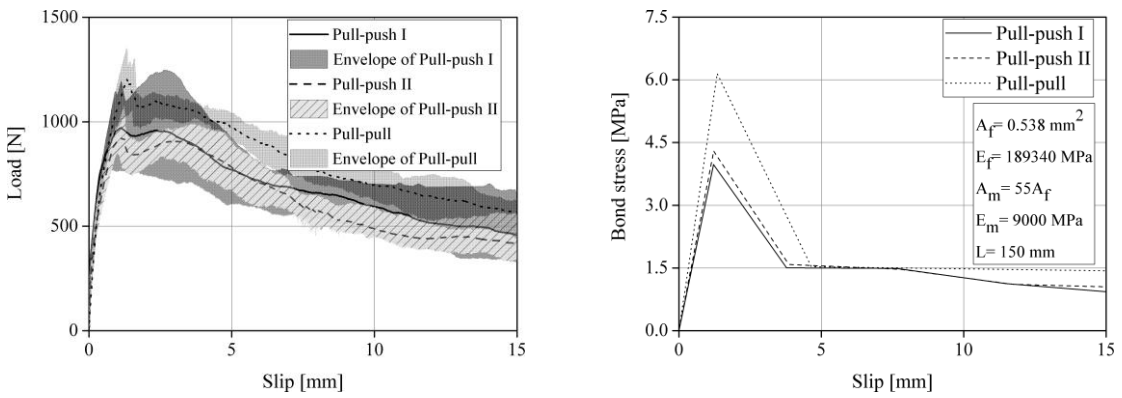

(a) (b)

Fig. 7. Effect of test setup on: (a) load-slip curves and (b) bond-slip laws.

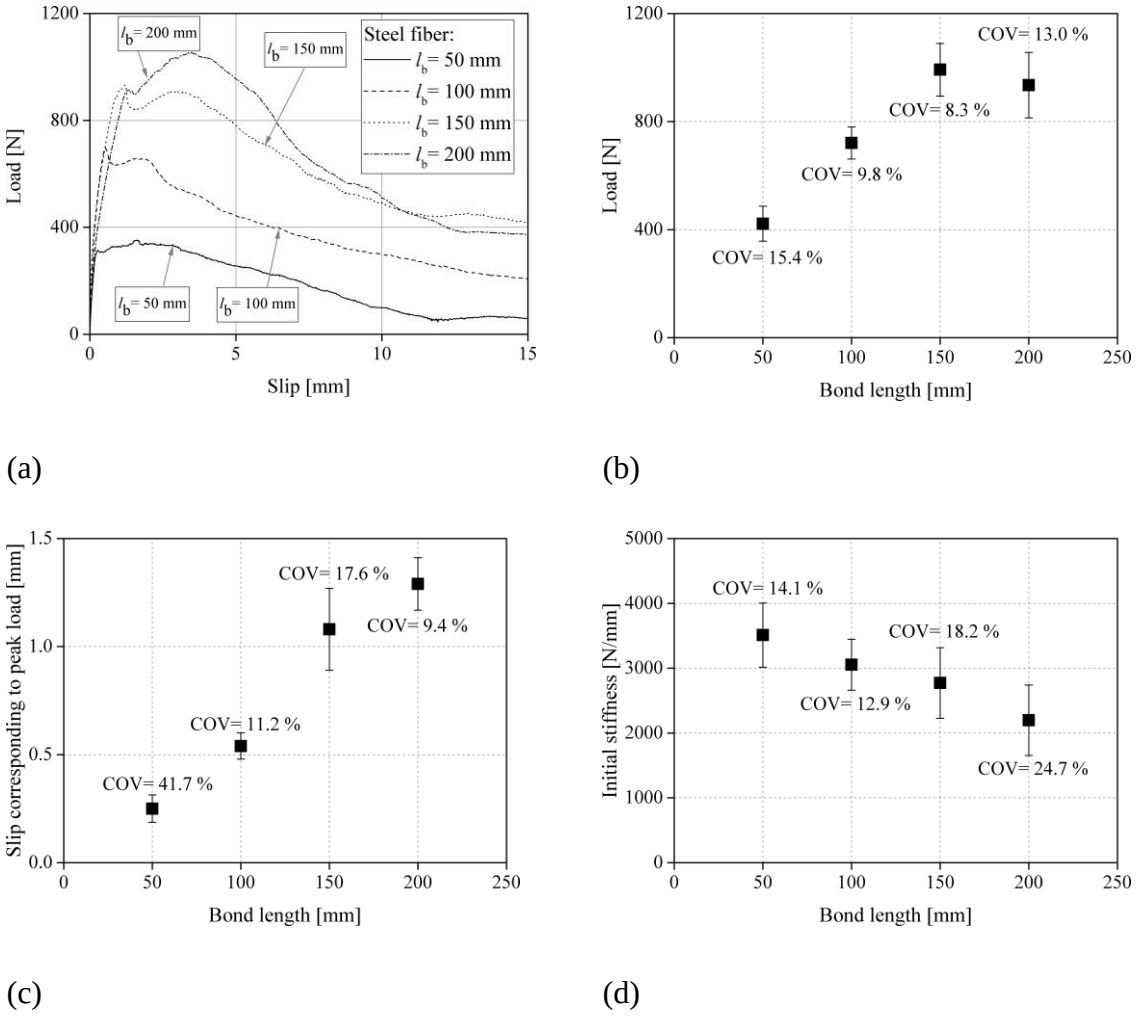

Fig. 8. Effect of embedded length on the pull-out response of Steel-based TRMs (a) average force-slip curves; (b) peak load; (c) slip corresponding to the peak load; (d) initial stiffness of the pull-out curves.

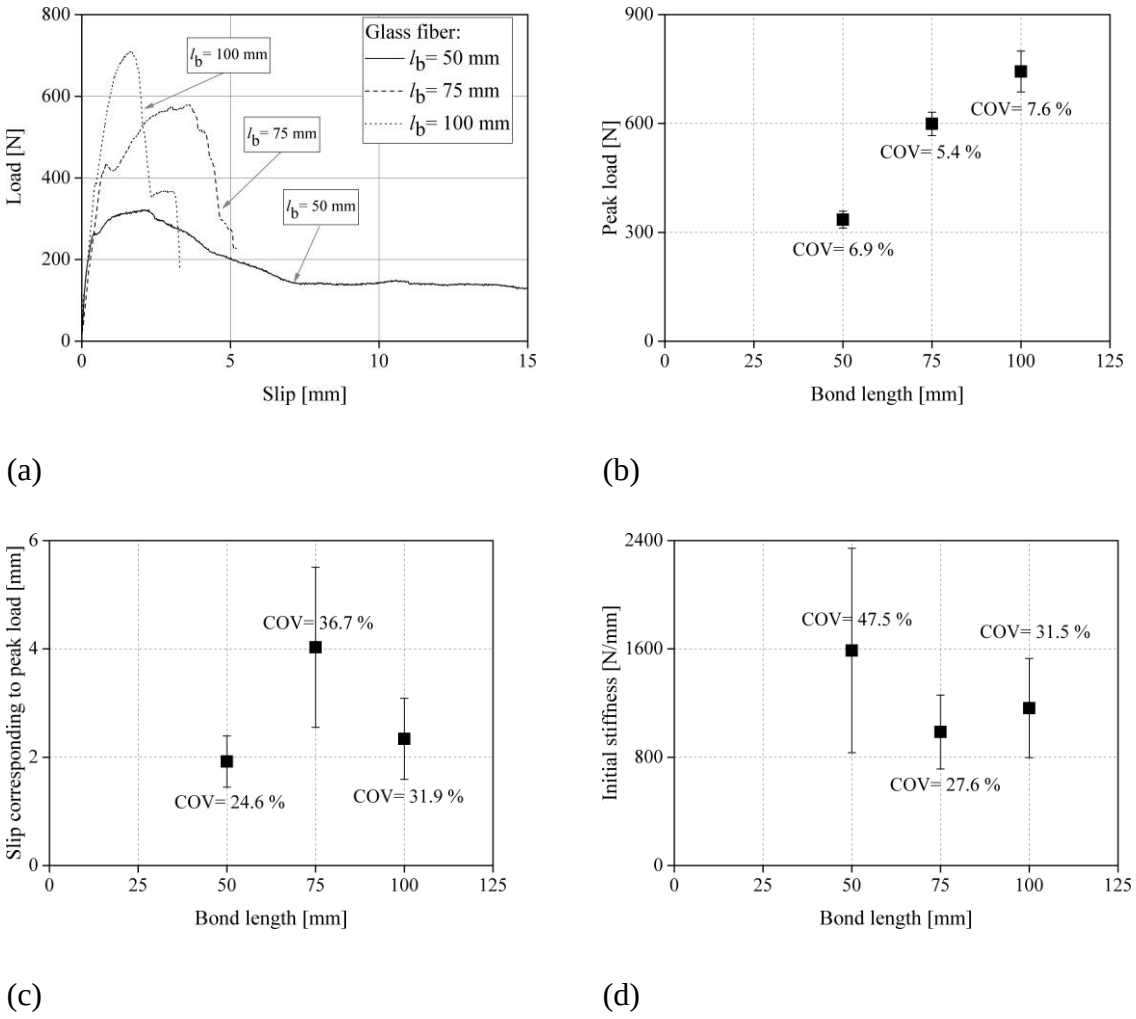

Fig. 9. Effect of fibre embedded length on the pull-out response of Glass-based TRMs (a) force-slip curves; (b) peak load; (c) slip corresponding to the peak load; (d) initial stiffness of the pull-out curves.

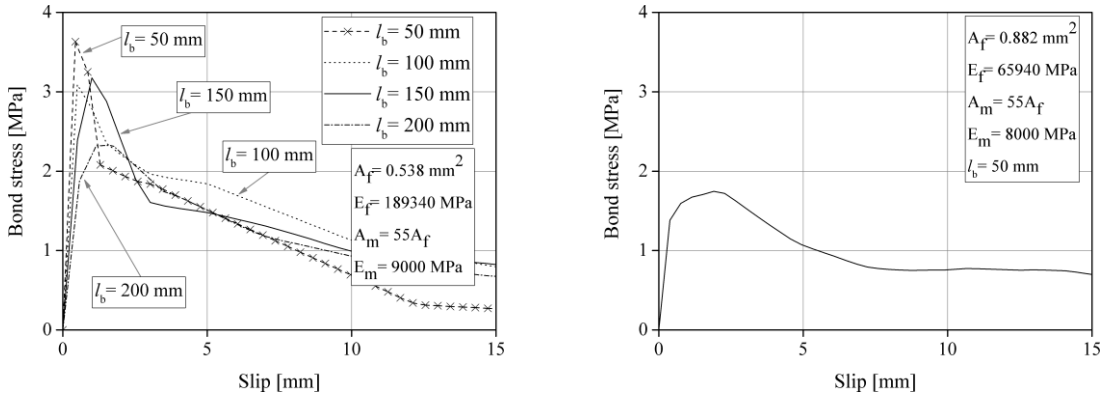

(a) (b)

Fig. 10. Effect of embedded length on bond-slip laws: (a) steel-based TRM and (b) glass-based TRM.

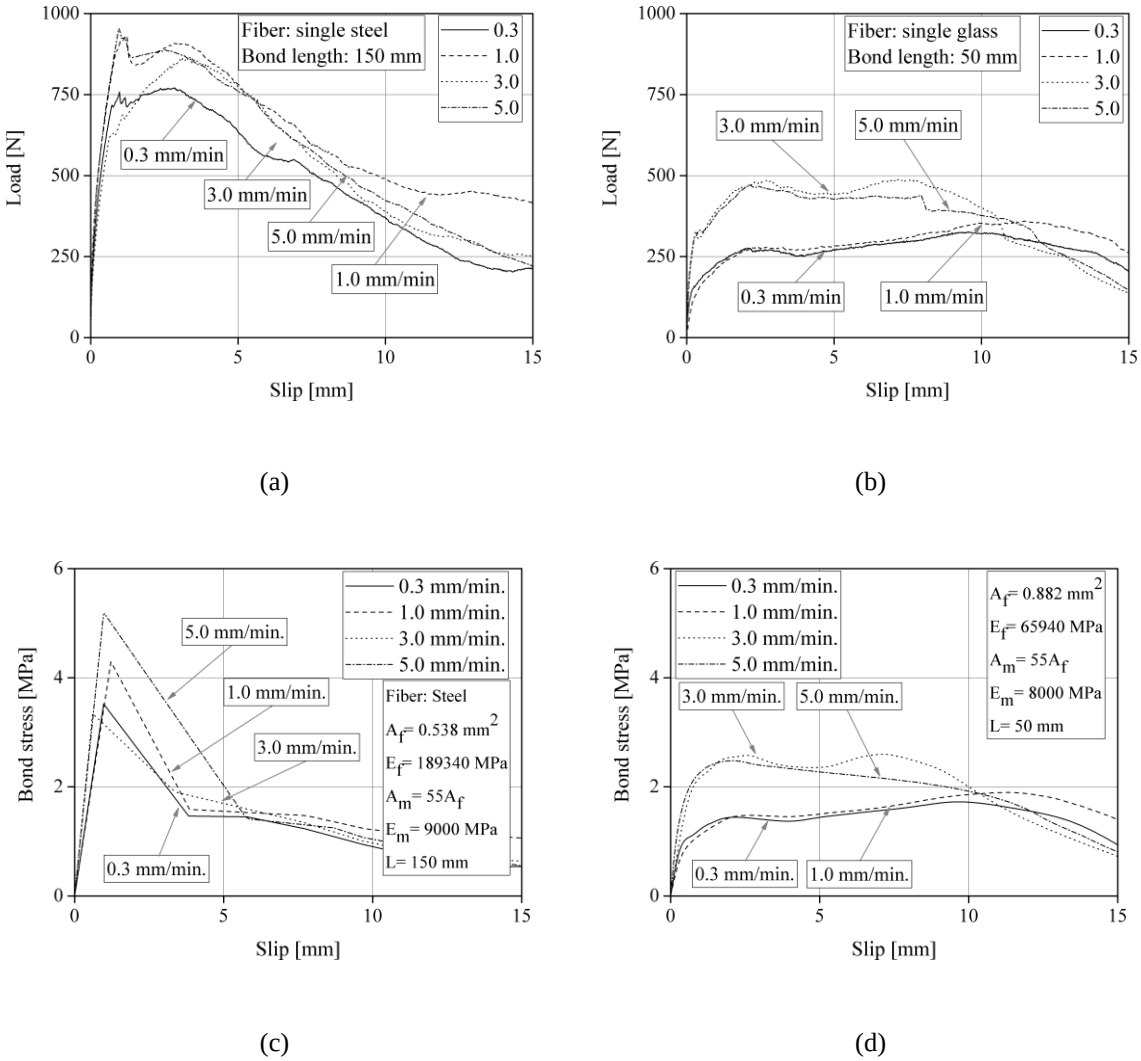

Fig. 11. Role of loading rate on the pull-out response of TRMs: (a) steel-based TRM; (b) glass-based TRM; (c) bond-slip law of steel-based TRM; (d) bond-slip law of glass-based TRM.

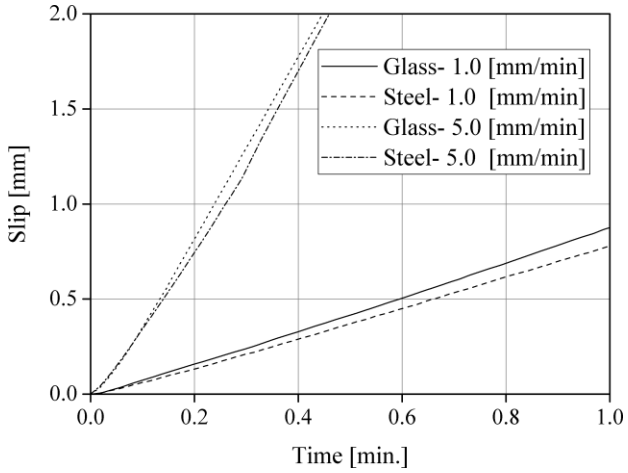

Fig. 12. Role of loading rate on the slip rate.

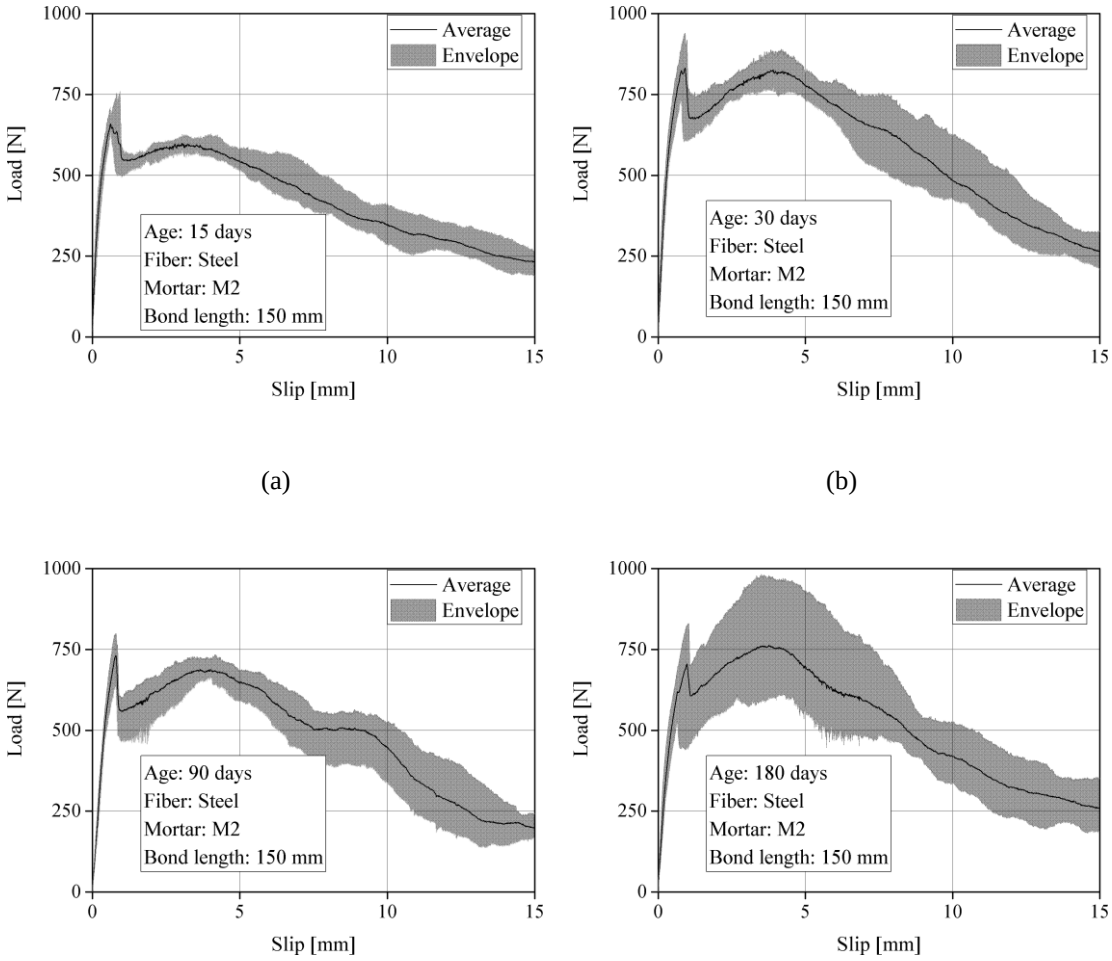

Fig. 13. Envelope and avergage load-slip curves of steel-based TRM at different mortar ages: (a)15 days; (b) 30 days; (c) 90 days; (d) 180 days.

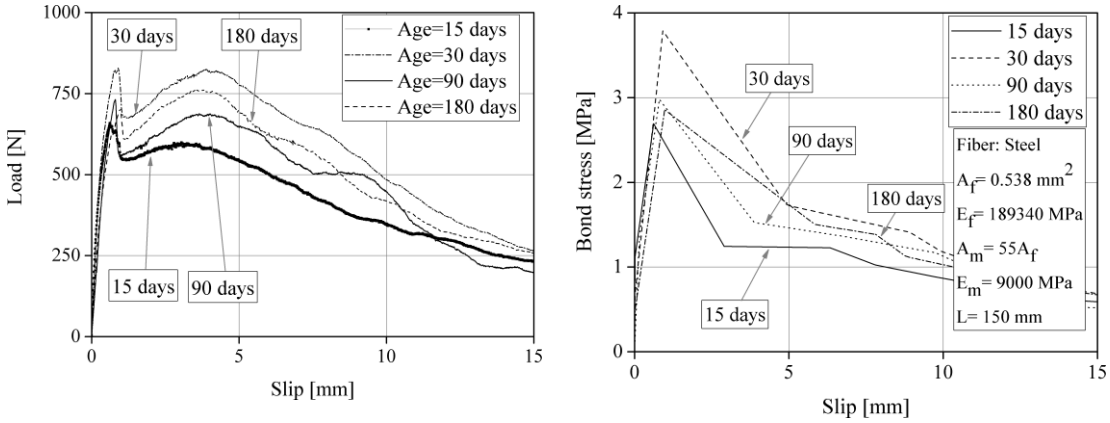

(a) (b)

Fig. 14. Role of mortar age on the pull-out response of Steel-based TRMs: (a) average pull-out curves; (b) average bond-slip laws.

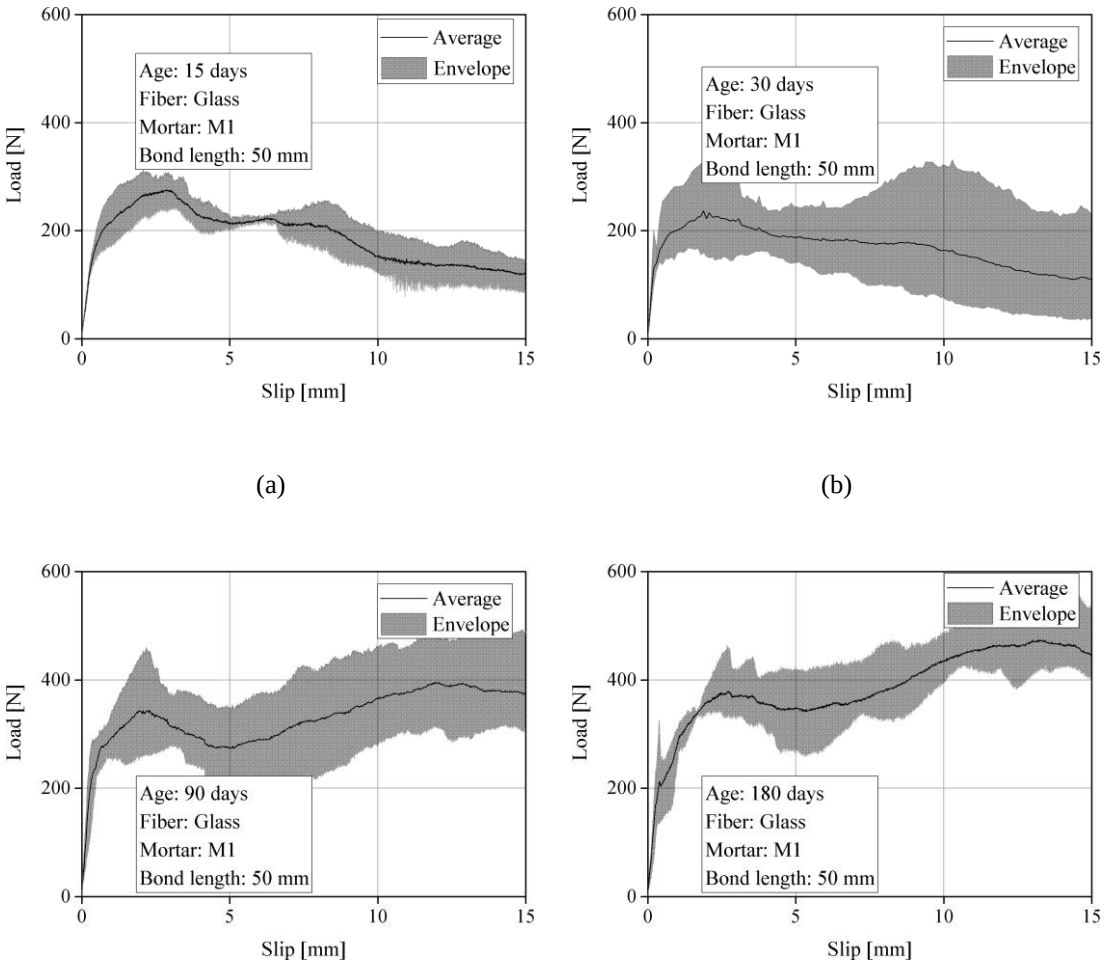

Fig. 15. Envelope and average load-slip curves of glass-based TRM at different mortar ages: (a) 15 days; (b) 30 days; (c) 90 days; (d) 180 days.

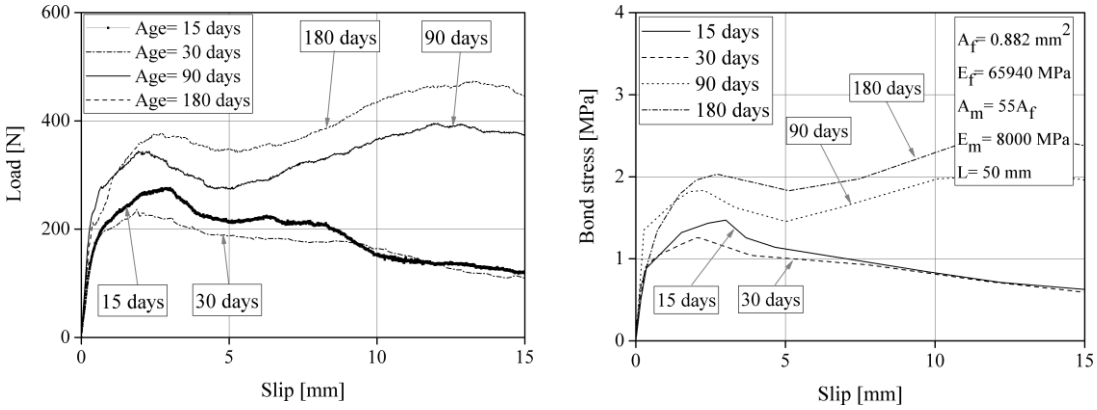

(a) (b)

Fig. 16. Role of mortar age on the pull-out response of glass-based TRMs: (a) average pull-out curves; (b) average bond-slip laws.

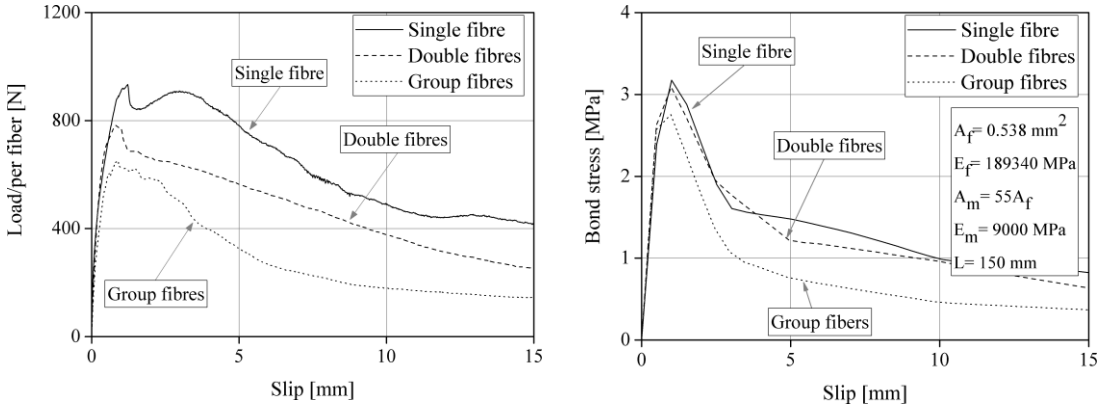

(a) (b)

Fig. 17. Role of fabric configuration on the pull-out response of steel-based TRMs: (a) average pull-out curves; (b) average bond-slip laws.

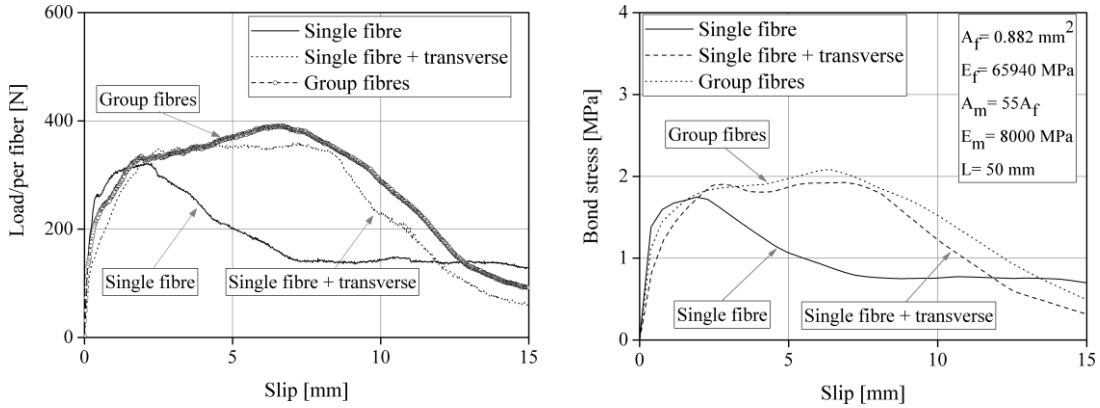

(a) (b)

Fig. 18. Role of fabric configuration on the pull-out response of glass-based TRMs: (a) average pull-out curves; (b) average bond-slip laws.

List of Tables

Table 1. Nomenclature for pull-out test specimens.

Test parameter	Fibre	Mortar	Bond length [mm]	Test setup	Age	Loading rate
Test setup	Steel	M2	150	I	60	1.0 mm/min
				II		
				III		
Load rate	Glass	M1	50	II	60	0.3 mm/min
						1.0 mm/min
						3.0 mm/min
						5.0 mm/min
	Steel	M2	100			0.3 mm/min
						1.0 mm/min
						3.0 mm/min
						5.0 mm/min
Embedded length	Glass	M1	50	II	60	1.0 mm/min
			75			
			100			
	Steel	M2	50			1.0 mm/min
			100			
			150			
			200			
Mortar age	Glass	M1	50	II	15	1.0 mm/min
					30	
					90	
					180	
	Steel	M2	150		15	1.0 mm/min
					30	
					90	
					180	
Fabric configuration	Glass	M1	50	II	60	1.0 mm/min
	Steel	M2	150	II	60	

Table 2. Mortar mechanical properties with age.

Mortar	Test	Mortar age [days]						
		3	7	14	28	60	90	180
M1	Compressive strength [MPa]	0.91 (4.5)	3.77 (5.4)	5.91 (9.2)	7.07 (10.5)	8.31 (12.2)	7.84 (4.7)	7.46 (11.3)
	Flexural strength [MPa]	-	2.51 (8.1)	4.03 (3.6)	4.71 (7.8)	5.10 (3.2)	4.66 (8.9)	6.00 (11.2)
M2	Compressive strength [MPa]	3.88 (8.5)	6.46 (7.8)	8.76 (7.8)	9.53 (11.1)	8.81 (13.8)	8.89 (5.9)	7.48 (10.3)
	Flexural strength [MPa]	1.40 (3.3)	1.53 (4.0)	1.79 (13.5)	2.54 (9.6)	2.09 (8.3)	2.33 (10.6)	2.62 (14.8)

Coefficients of variation (%) are provided in parentheses.

Table 3. Role of test setup on the pull-out response (steel-based TRM).

Test setup	Peak load [N]	Slip corresponding to peak load [mm]	Toughness at a crack opening of [N.mm]			Initial stiffness [N/mm]
			1 mm	4 mm	8 mm	
Pull-push I	987 (21.8)	0.78 (40.7)	720.0 (6.7)	3270.3 (9.4)	6050.8 (10.2)	1762 (9.9)
Pull-push II	992 (9.8)	1.08 (17.6)	649.0 (9.5)	3224.6 (6.5)	5982.9 (8.9)	2772 (18.2)
Pull-pull	1245 (12.5)	1.33 (20.8)	692.4 (7.2)	3950.8 (4.3)	7554.4 (5.3)	2032 (27.3)

Coefficients of variation (%) are provided in parentheses.

Table 4. Role of loading rate on the pull-out response of steel-based TRM.

Load rate [mm/min]	Peak load [N]	Slip corresponding to peak load [mm]	Toughness at a crack opening of [N.mm]			Initial stiffness [N/mm]
			1 mm	4 mm	8 mm	
0.3	810 (24.7)	0.9 (27.4)	552.4 (14.0)	2786.8 (11.6)	5112.7 (16.0)	1250.3 (18.3)
1.0	993 (9.8)	1.1 (17.6)	646.2 (9.3)	3295.1 (7.7)	6137.4 (9.7)	2993.9 (18.2)
3.0	694 (27.0)	0.8 (27.3)	488.4 (16.7)	2880.9 (12.3)	5626.0 (12.9)	1505.4 (26.4)
5.0	1007 (9.4)	1.1 (10.7)	651.9 (5.6)	3268.9 (8.9)	5999.9 (8.1)	2504.8 (33.9)

Table 5. Role of loading rate on the pull-out response of glass-based TRM.

Load rate [mm/min]	Peak load [N]	Slip corresponding to peak load [mm]	Toughness at a crack opening of [N.mm]			Initial stiffness [N/mm]
			1 mm	4 mm	8 mm	
0.3	304 (25.4)	2.4 (28.9)	174.3 (33.7)	954.9 (30.0)	2076.8 (30.3)	858.5 (32.9)
1.0	311 (10.6)	2.8 (29.3)	148.9 (26.9)	940.5 (11.1)	2110.7 (10.0)	645.9 (31.5)
3.0	504 (8.9)	2.5 (25.5)	305.7 (11.6)	1681.3 (7.7)	3534.7 (9.9)	1322.5 (36.3)
5.0	499 (10.9)	2.8 (26.5)	306.3 (4.6)	1637.1 (7.1)	3364.3 (11.8)	3193.8 (39.5)

Table 6. Role of mortar age on the pull-out response of steel-based TRM.

Age [days]	Peak load [N]	Slip corresponding to peak load [mm]	Toughness at a crack opening of [N.mm]			Initial stiffness [N/mm]
			1 mm	4 mm	8 mm	
15	720 (7.4)	0.8 (18.6)	511.3 (9.3)	2238.3 (4.5)	4235.7 (5.9)	2410 (43.2)
30	871 (10.9)	0.9 (11.0)	599.5 (11.4)	2861.0 (5.9)	5745.4 (6.9)	2147 (33.3)
90	740 (9.9)	0.8 (3.3)	474.2 (9.7)	2372.0 (8.5)	4747.0 (8.2)	1289 (16.8)
180	730 (19.4)	0.9 (18.9)	476.5 (18.3)	2580.5 (17.6)	5143.2 (19.6)	1520 (31.2)

Coefficients of variation (%) are provided in parentheses.

Table 7. Role of mortar age on the pull-out response of glass-based TRM.

Age [days]	Peak load [N]	Slip corresponding to peak load [mm]	Toughness at a crack opening of [N.mm]			Initial stiffness [N/mm]
			1 mm	4 mm	8 mm	
15	284 (12.1)	2.6 (14.0)	153.8 (13.0)	913.8 (11.3)	1778.4 (4.4)	482 (16.8)
30	250 (34.8)	1.9 (35.8)	156.4 (21.3)	804.4 (27.5)	1540.2 (30.7)	639 (30.8)
90	378 (18.2)	2.3 (15.3)	227.3 (10.2)	1226.8 (13.6)	2476.5 (18.8)	856 (24.4)
180	390 (13.7)	2.3 (31.1)	190.8 (19.6)	1251.8 (3.7)	2672.6 (10.1)	781 (20.3)

Coefficients of variation (%) are provided in parentheses.

Table 8. Role of fibre configuration on the pull-out response of steel-based TRM.

Configuration	Peak load [N]	Slip corresponding to peak load [mm]	Toughness at a crack opening of [N.mm]			Initial stiffness [N/mm]
			1 mm	4 mm	8 mm	
Single cord	992 (9.8)	1.08 (17.6)	646.2 (9.3)	3295.1 (7.7)	6137.4 (9.7)	2772 (18.2)
Two cords	815 (14.2)	0.89 (26)	617.8 (9.3)	2573.7 (14.1)	4684.2 (17.6)	2863 (30.3)
4 cords	700 (15)	0.74 (43.8)	494.4 (20.8)	2086.3 (14.6)	3219.9 (25.7)	2058 (61.6)

Coefficients of variation (%) are provided in parentheses.

Table 9. Role of fibre configuration on the pull-out response of glass-based TRM.

Configuration	Peak load [N]	Slip corresponding to peak load [mm]	Toughness at a crack opening of [N.mm]			Initial stiffness [N/mm]
			1 mm	4 mm	8 mm	
Single roving	335 (6.9)	1.92 (24.6)	238.1 (12.3)	1118.2 (8.9)	1825.9 (8.9)	1588 (47.5)
Single roving+transverse elements	367 (7.6)	2.93 (17.5)	162.6 (14.8)	1137.5 (8.7)	2545.2 (5.2)	795 (29.5)
Two rovings+transverse elements	404 (8.1)	7.05 (17.8)	206.0 (13.8)	1193.4 (7.2)	2695.2 (8.6)	1238 (28.2)

Coefficients of variation (%) are provided in parentheses.